

Photon Emission during Deformation of Glass-Fiber-Reinforced Bisphenol-A-Polycarbonate*

JÜRGEN FUHRMANN,^{1,†} LEO NICK,¹ J. THOMAS DICKINSON,² and LESLIE C. JENSEN²

¹Institut für Physikalische Chemie, Technische Universität Clausthal, Arnold-Sommerfeld-Str. 4, 3392 Clausthal-Zellerfeld, Germany; ²Department of Physics, Washington State University, Pullman, Washington 99764-2874

SYNOPSIS

We give a survey on mechanically induced emission phenomena (acoustic emission [AE], neutral particle emission [NE], electron and charged particle emission [EE/PIE], radio wave emission [RE]) of polymers and briefly summarize these effects in unfilled and glass-fiber-reinforced bisphenol-A-polycarbonate. A general treatment of the photon emission kinetics in terms of analysis and description, using a convolution function, is proposed. The kinetics obey a power law decay in time. By examining a model mechanism for the interfacial failure of the composite, i.e., by peeling of glass/polymer laminates, we show that the origin of the photon emission is the polycarbonate matrix after cleavage of the glass/polymer interface. Spectral characteristics of mechanically induced luminescence of glass-filled polycarbonate and of the peeling spectra of the model system of glass/polycarbonate laminates are discussed. Different brands of polycarbonate yield identical spectra. Spectra recorded during peeling in vacuum are very similar to those recorded during deformation of the composite. Polarized fluorescence spectroscopy and electron-beam luminescence were used to obtain further information about the intrinsic polycarbonate-chromophores that are available for mechanically induced photon emissions. © 1993 John Wiley & Sons, Inc.

MECHANICALLY INDUCED EMISSION PHENOMENA

During mechanical stimulation, a variety of emission phenomena, like acoustic emissions, emissions of neutral, and positively or negatively charged particles, respectively, as well as photons and radio waves may be observed (Table I).

The mechanical stimulation, usually uniaxial deformation, may be subdivided into three regimes:

- (i) elastic deformation, i.e., the linear, "Hookian" region of the stress-strain curve;
- (ii) plastic deformation, e.g., neck formation and neck propagation; and
- (iii) macroscopic fracture of the sample as the final state of deformation.

Emissions that are observed in regime (iii) are summarized by the term "fracto-emission." When may we expect to observe emissions and which are the physical characteristics to be measured?

Acoustic Waves

Whenever fast relaxations of elastically stored deformation energy occur, acoustic waves may be observed. The dimensions of the relaxing sample volumes have to be large enough so that the equations of macroscopic continuum mechanics can be applied. These requirements are found in heterogeneous media at the transition from elastic to plastic behavior. The basic measuring parameters are the emission kinetics (events vs. time) and, with some assumptions on the damping properties of the material and the spatial distribution of the emitting sites, the released energy. Frequency (spectral) information is principally also available, but due to prominent resonance effects in acoustic detectors, it difficult to interpret.¹ The acoustic emission results mentioned

* Manuscript of a lecture given at the 3rd Dresden Polymer Discussion, Gaussig, Germany, April 1991.

† To whom correspondence should be addressed.

Table I Mechanically Induced Emission Phenomena—Overview

Mechanical Stimulation	Elastic Deformation	Plastic Deformation	Fracture
Photons	—	Kinetics, Spectra	
Neutral particles	—	Mass analysis → Chemical species	
Charged particles	—	Kinetics, Spectra [Mass analysis]	
Acoustic waves	—	Kinetics, Energy [Spectra]	—
Radio waves	—	Gas discharge?	

in this paper were obtained at the German Polymer Institute (DKI, Deutsches Kunststoff Institut) in Darmstadt.^{2,3}

Neutral Particles

The neutral particles are small, volatile molecules that are products of mechanochemical degradation of the polymer, which are split off from thermodynamically unstable primary products of macromolecular bond cleavages during plastic deformation and fracture. The mass analysis of these fragments leads to conclusions about their chemical species and information about the reaction paths involved in mechanochemical polymer degradation. Neutral particles may be expected whenever bond-cleavage reactions occur, i.e., whenever the mechanical stress concentration in the material rises above a critical, temperature-dependent and polymer-specific value.

One note of caution: Polymers generally contain a number of trapped gases that basically “degas” from the freshly formed fracture surface. As pointed out by Grayson and Wolf,⁴ one must carefully distinguish between those occluded in the specimen and those resulting from bond scissions. The latter is fundamentally more interesting and intimately related to the energetics of fracture, although the former (occluded gas) can, in fact, be useful for characterizing the failure of materials.⁵

Charged Particles

Electrons and positively or negatively charged ions may be detected. During deformation, we found them always to be correlated with molecular fracture events. At the macroscopic fracture of heterogeneous materials, gas discharge phenomena may also lead to ionic species or electrons.⁶ The emission kinetics and the energy distribution of the emitted particles

may be measured. In principle, a mass analysis of the ionic emission is possible by time-of-flight or quadrupole mass spectroscopy, although high kinetic energies or uncertainties in the time-of-flight trigger often result in large uncertainties in the masses.⁶⁻⁸

Photons

There are several mechanisms of photon emissions to be discussed. The mechanochemical bond cleavage that leads to neutral and charged particle emission may also result in excited states that relax to the ground state by photon emission.⁹ Fracture of heterogeneous materials can result in gaseous discharges and the observed photons may be a gas discharge luminescence or a luminescence of the fracture surface that is stimulated by irradiation or particle bombardment by the discharge plasma.⁶ A fourth possibility to discuss is that the photon emission is generated by cleavage of adhesive contacts without gas discharge phenomena. We will show that the mechanically induced photon emission of glass-filled polycarbonate belongs to this last type. The basic experimental data are the emission kinetics and the spectral distribution of the photons.

Radio Waves

Radio waves are generally observable accompanying gas discharges. We will use the issue of their observation as a test for the occurrence of gas discharge processes only.

UNFILLED BISPHENOL-A-POLYCARBONATE

In polycarbonate, the plastic deformation process is “diffuse shearing,”¹⁰ i.e., the process is a pure shearing deformation, but without formation of distinct

shear bands. A necking region forms and moves through the sample during deformation. The stress distribution in the necking region is fairly uniform.

The main features of the mechanically induced emission phenomena of neat polycarbonate (Makrolon™ 2800, Bayer and Calibre™ 300-10, Dow) are (Table II) the following:

Acoustic Waves²

No acoustic emissions are observed during deformation of the unfilled material, as can be expected because there are no heterogeneities like microcracks and crazes of sufficiently large dimensions (in the order of magnitude of microns) to allow for sudden relaxations of elastic deformation energy.

Neutral Particles¹¹

No neutral particles that can be attributed to bond breaking were detected during elastic deformation and necking, but at macroscopic fracture of the samples, carbon monoxide and perhaps carbon dioxide (masses 28 and 44) evolve. No characteristic mass fragments of the bisphenol-A-system (e.g., masses 39, 41, and 91) were found. This is consistent with a C—O single-bond cleavage in the carbonate group under mechanical activation. The primary fragments are unstable and split off CO and CO₂ to form the more stable phenoxy and phenyl radicals, respectively. In very clean polycarbonate films, the evolved amount of CO₂ is very low,¹² i.e., the reaction path leading to CO and phenoxy radicals is favored. These mechanisms are similar to proposed mechanisms for radiative degradation of polycarbonate.¹³

Charged Particles¹⁴⁻¹⁶

The emission behavior of positively and negatively charged particles is similar to the neutral emission

characteristics, as can be expected from their common origin in molecular fracture events. No charged particles were detected during elastic deformation and necking, but at macroscopic fracture, a fast decaying (α 10 ms) burst of both positively and negatively charged particles was observed. The emission intensities of both the positively and negatively charged particles were similar. On submicrosecond time scales, the onset of *EE* was found to correspond to a crack velocity of ~ 5 m/s and the peak emission intensity occurs at the completion of fracture.

Photons¹⁴⁻¹⁶

Very weak photon emission was observed at the onset of neck formation and during fracture of the unfilled polycarbonate, the latter showing similar behavior to the electron emission, rising during slow crack growth and most intense during rapid (macroscopic) fracture.

Radio Waves

The occurrence of radio waves was not examined in unfilled polycarbonate; our prediction would be that little or no long wavelength radiation would occur during deformation and fracture.

GLASS-FIBER-REINFORCED BISPHENOL-A-POLYCARBONATE

For these investigations, the neat polycarbonate (Makrolon 2800) was filled with 10 wt % untreated E-glass fibers of 10 μ m diameter and 100 μ m average length. Whereas the basic deformation mechanism remains a shear process, the incorporation of filler particles results in highly nonuniform stress concentrations in the vicinity of the fillers. Matrix cracks, matrix/filler dewetting, and fiber pullout

Table II Mechanically Induced Emission Phenomena—Unfilled Polycarbonate

Mechanical Stimulation	Elastic Deformation	Necking Process: "Diffuse Shearing"	Fracture
Photons	—	Very small	Small
Neutral particles	—	—	CO, CO ₂ (small)
Charged particles	—	Very small	Positive and negative
Acoustic waves	—	—	—
Radio waves	—	Not examined	—

occur in the plastic deformation regime, which—macroscopically—still involves necking. The observed emission phenomena (summarized in Table III) differ considerably from the unfilled material:

Acoustic Waves^{2,3}

Acoustic emissions are observed prior to neck formation where the mode of deformation changes from elastic to plastic and both processes contribute to energy storage and dissipation. The cracking, dewetting, and fiber pullout events are sufficiently large in the involved volume and sufficiently discrete to produce acoustic waves. In the plastic regime of neck propagation, acoustic emissions vanish.

Neutral Particles

The issue of the emission of neutral particles from the filled polycarbonate has not (yet) been investigated.

Charged Particles^{14,15}

No charged particle emission has been observed in the elastic regime of the stress-strain curve. Emissions of both negatively and positively charged particles start with neck formation and persist during neck propagation, macroscopic fracture, and, due to relaxation processes within the polycarbonate matrix, even several hours after fracture or after partial deformation without macroscopic fracture of the sample. The stress-concentrating effect of the filler particles is sufficient to overcome the activation barrier of mechanochemical bond cleavage. We will not elaborate on this phenomenon in the present paper. A detailed analysis may be found in the cited literature (Refs. 14 and 15). In particulate-filled

elastomers, similar emissions were attributed to dewetting events occurring on the exposed surface of the sample¹⁷ prior to fracture. After fracture, surfaces having experienced detachment (interfacial failure) would also yield long lasting postfracture emissions. A detailed analysis of particle emission during deformation of unfilled natural rubber proved the molecular fracture origin of particle emission in this system.¹⁸

Photons

Intense photon emission occurs during neck propagation and fracture, but was observed neither before neck formation nor after the fracture emission decay. The existence of an intense mechanically induced photon emission in filled polycarbonate and its very weak intensity in the case of the unfilled material indicates the dramatic effect of interfaces in the emission process^{14,19,20} leading to these high intensities. The missing analogy of the intense photon emission to the particle emission behavior in terms of kinetics and intensity in the different materials—again—indicates that luminescence after a molecular fracture reaction^{9,14} is not the direct photon-generating mechanism for the high intensities, but it is probably involved in the low-intensity part detected in the unfilled polycarbonate. A detailed discussion of the kinetic and spectral photon emission characteristics will follow in the main part of this paper.

Radio Waves

Radio waves were observed neither during elastic deformation and necking nor at macroscopic fracture of the samples, i.e., no evidences for gas discharges were found.

Table III Mechanically Induced Emission Phenomena—Glass-reinforced Polycarbonate

Mechanical Stimulation	Elastic Deformation	Necking	Fracture	Long-time Relaxation After Fracture
Photons	—	Observed	Observed	—
Neutral particles		Not examined		
Charged particles	—	Positive and negative	Positive and negative	Positive and negative
Acoustic waves	—	Observed		—
Radio waves	—	—	—	—

PHOTON EMISSION KINETICS

Figure 1 shows the photon emission rate vs. time during deformation of glass fiber-reinforced polycarbonate. The dashed line gives a sketch of the load on the sample. The photon emission rate rises above the dark count level with the beginning of neck formation. It stays on a nearly constant level during neck propagation, has a slight maximum at fracture, and decays to the dark count level.

A general description of the kinetics is obtained by a convolution ansatz:

$$E(t) = \int_{\Theta=-\infty}^t A(\Theta) \cdot R(t - \Theta) d\Theta$$

t , Θ is time; $E(t)$, photon emission rate; $A(\Theta)$, excitation function; and $R(t - \Theta)$ relaxation function.

The excitation function may be identified with neck propagation, i.e., $A(t) = 0$ before neck formation, $A(t) \approx \text{constant}$ during the constant-velocity neck propagation, and $A(t) = 0$ after fracture.

The relaxation function $R(t)$ may be estimated by the emission decay kinetics after fracture. This decay can satisfyingly be described by the power law:

$$R(t) = a \cdot \left[\frac{t}{t^+} \right]^{-n}; \quad t^+ \text{ unit time (1 s)}$$

Typical fit parameters are $a = 15,000$ (counts per second) and $n = 0.85$. The exponent n can be interpreted as a coupling parameter among the relaxing, the photon emitting site, and the simultaneously relaxing complex environment. A value of 0 would indicate an uncoupled system, and a value of 1, a perfectly coupled system.²¹

In addition to the formal description of the emission kinetics, the convolution ansatz can be used for analytical purposes. If an estimation of the relaxation function $R(t)$ is available, e.g., by the above-demonstrated fit to a decay after stimulation, a deconvolution of the measured emission kinetics $E(t)$ and this relaxation function $R(t)$ renders the "true" excitation function.

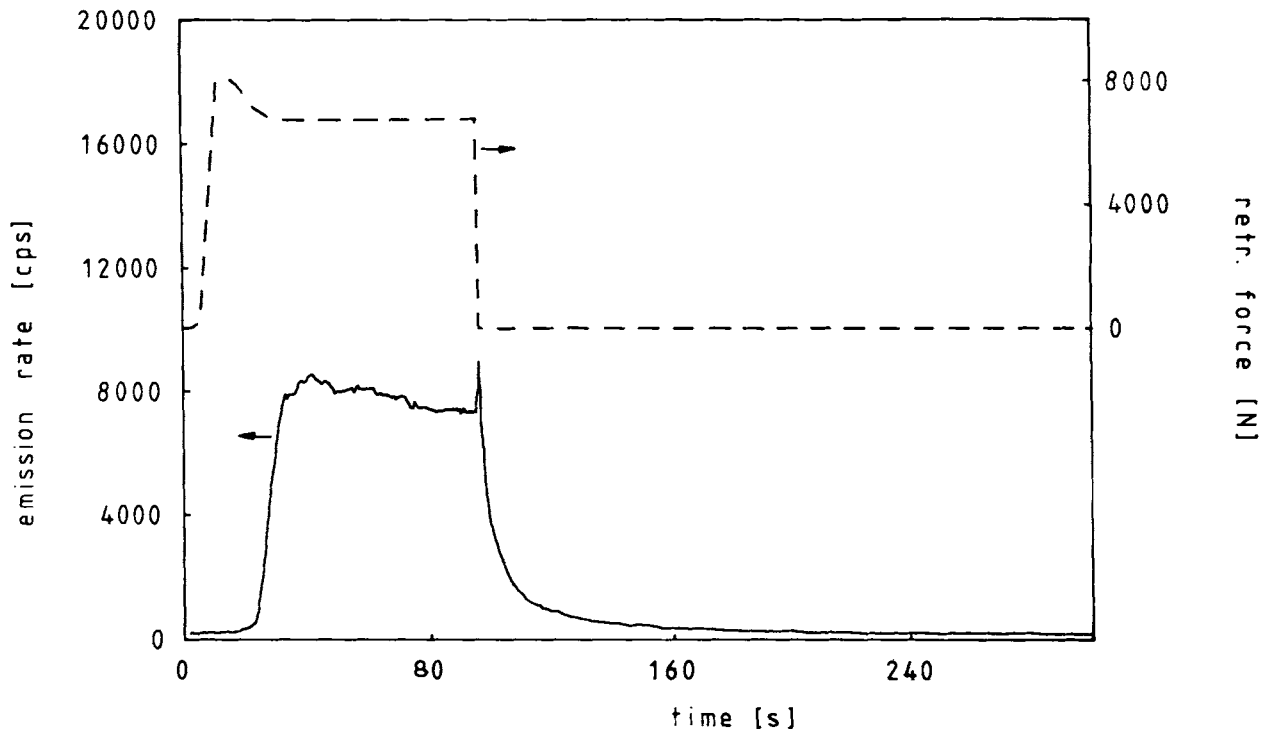


Figure 1 Photon emission rate and load vs. time. Sample: bisphenol-A-polycarbonate, Makrolon 2800, Bayer with 10 wt % untreated E-glass fibers (length $\sim 100 \mu\text{m}$, diameter $10 \mu\text{m}$) injection-molded dumbbell $40 \times 5 \times 2 \text{ mm}^3$. Deformation rate: 12 mm/min. (—) Photon emission rate (counts per second); (---) load on the sample (Newton).

PHOTON EMISSION ORIGIN¹¹

Intense photon emissions were observed *only* in glass-filled polycarbonate and no evidences for gas discharges were found. Therefore, the hypothesis evolved that the intense photon emissions are a luminescence "involving the glass/polycarbonate interface." In the neat material, the bond scissions accompanying fracture are responsible for the weak, but measurable photon emission by chemiluminescence effects or by radiative recombination^{14,16} of states excited by the fracture process.

To investigate the interface properties, we designed a model system: solvent-cast films (thickness $\sim 20 \mu\text{m}$) of polycarbonate on microscope glass slides. Coming out of the interface, there are still three possibilities for the photon emission origin: It could be the interface itself, i.e., the two dissimilar

materials in close contact, or it could be either material, glass or polycarbonate, after cleavage of the contact. The following experiments (Fig. 2) provided the answer:

We performed two types of peeling experiments as shown in Figure 2(a) and (b). In both, a glass slide/polycarbonate laminate was positioned in front of a photon detector (PMT). In the first experiment, we peeled the polycarbonate film only partially off the glass slide. It still adhered at one side and stayed horizontally in front of the PMT. In the second type of experiment, we peeled the polycarbonate film totally off and quickly moved it out of the sensitivity horizon of the photon detector. The respective emission rates (log scale) are shown in Figure 2(c) and (d).

If the film stays in front of the PMT, a sudden rise in the emission rate at the moment of peeling,

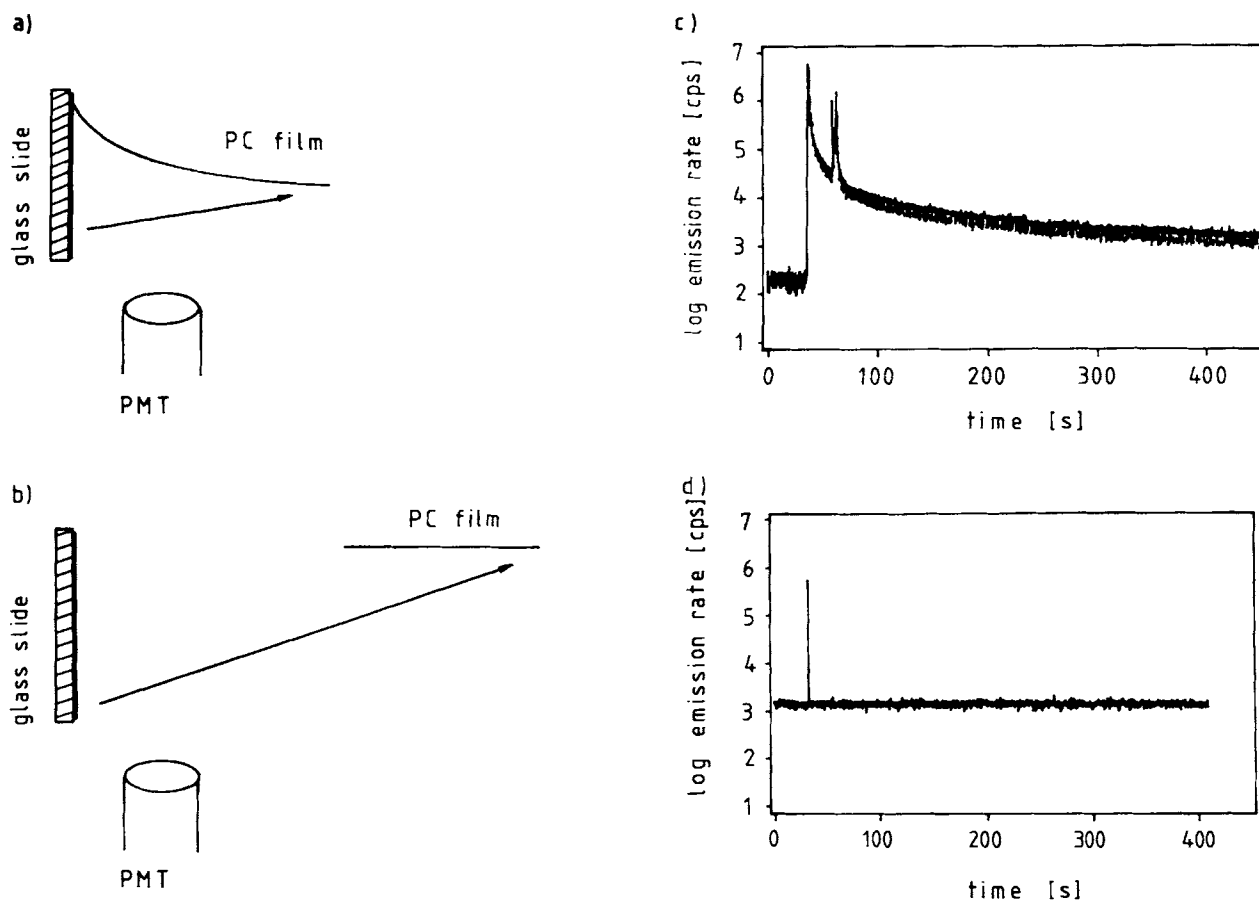


Figure 2 Setup and photon emission kinetics in peel experiments. Sample: solvent-cast film of bisphenol-A-polycarbonate (Calibre 300-10) on glass-slides (polycarbonate/glass laminate). (a) Setup, in which the polycarbonate film after peeling stays in front of the photon detector (PMT); (b) setup, in which the polycarbonate film after peeling is moved out of the sensitivity horizon of the photon detector; (c) photon emission kinetics of setup (a); (d) photon emission kinetics of setup (b).

which then decays over several hundred seconds, is observed [Fig. 2(c)]. The second emission maximum, visible in Figure 2(c), was produced by a further peeling, due to relaxations in the peeled film.

If the film is immediately moved out of the sensitive area of the PMT after peeling, only a sharp emission peak at the moment of peeling, less than 300 ms wide, is observed. This result unambiguously shows that the polycarbonate is the luminescent material. The glass slide, which stays in front of the photon detector, gives no contribution to the photon emission phenomenon.

SPECTRAL DISTRIBUTION¹¹

The mechanically induced emission spectra were recorded using optical multichannel analyzer techniques. Figure 3 shows the spectra of the luminescence during deformation of the glass fiber-reinforced polycarbonate in vacuum and in air.

The spectrum in vacuum was recorded by using an optical fiber feed between sample and spectrograph. Spectral intensity was available only while the necking region crossed the optical fiber end. The spectrum consists of a very broad, unstructured band in the wavelength region from ~ 220 to ~ 800 nm with a maximum around 375 nm. The emissions below 290 nm are in the absorbing spectral region of polycarbonate. This implies that this part of the emission has to come out of regions close to the sur-

face of the material where reabsorption is of no importance. No evidence for underlying narrow emission lines are found that would be typical for gas discharges produced by fracture.²²

The spectrum of the luminescence during deformation in air is similar. The emission starts, about 70 nm higher on the wavelength scale than the "vacuum spectrum" at ~ 290 nm, has a maximum at 425 nm and extends to ~ 850 nm. A shoulder at 620 nm is observed.

The spectra recorded during peeling of the model system of glass/polycarbonate laminates are shown in Figure 4. Especially, the peeling spectrum recorded in vacuum [Fig. 4(a)] is very similar to the deformation-induced spectra of the glass-filled polycarbonate (Fig. 3): The emission extends from ~ 220 to ~ 800 nm with a maximum at 375 nm. A second maximum emerges around 550 nm. The similarity of this vacuum spectrum to both spectra of the glass-filled material can be explained by the near-vacuum conditions at most sites of adhesive failure, even if the sample—macroscopically—is under normal pressure in air. This work is another example of using photons to probe failure at interfaces embedded within a matrix.²³⁻²⁵

The peeling spectra of two different brands of polycarbonate [Makrolon 2800, Bayer and Calibre 300-10, Dow; Fig. 4(b) and (c)] in air are found to be nearly identical. Emission starts at ~ 290 nm, as in the glass-filled polycarbonate in air, but there are two distinct bands to be observed with the max-

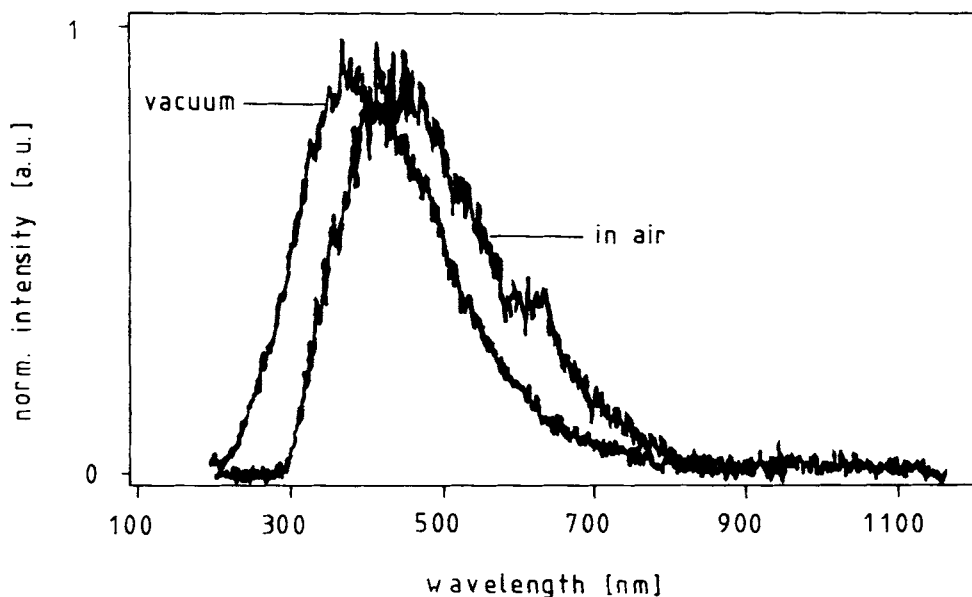


Figure 3 Luminescence spectra of glass fiber-reinforced polycarbonate during deformation. Sample: identical to Fig. 1. Vacuum: 10^{-4} Pa.

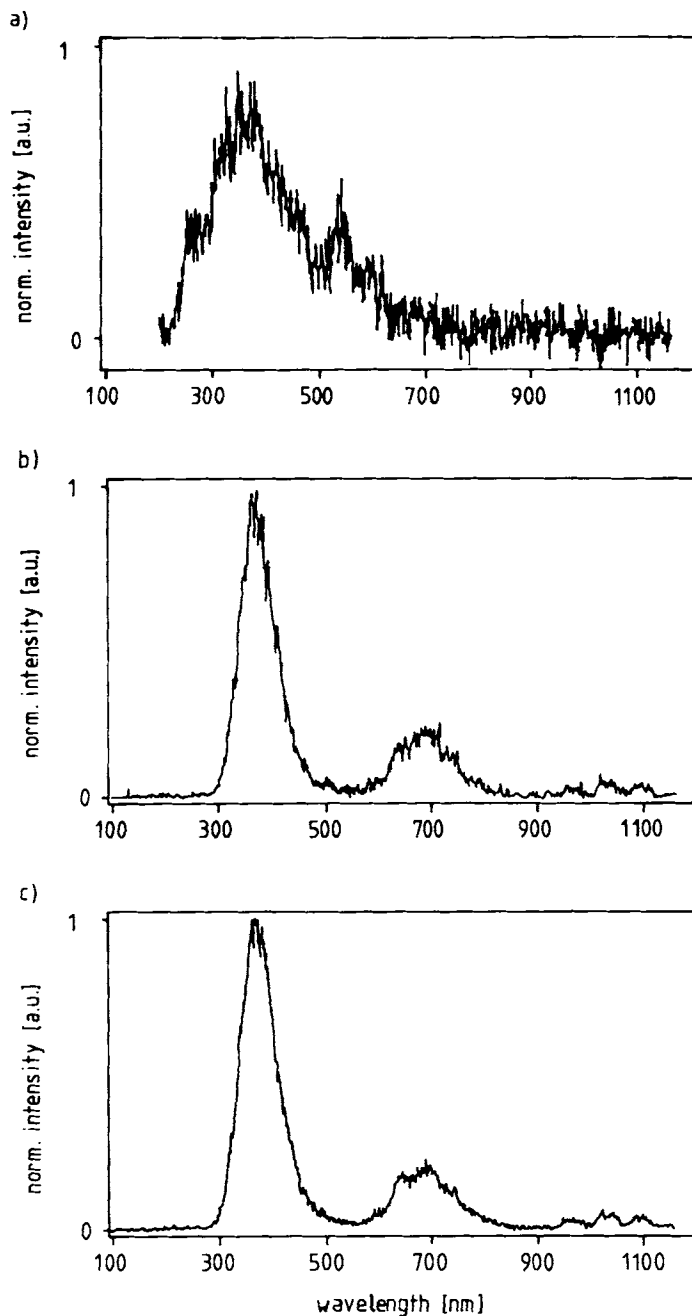


Figure 4 Peeling luminescence spectra of glass/polycarbonate laminates: (a) polycarbonate Calibre 300-10 in vacuum; (b) polycarbonate Calibre 300-10 in air; (c) polycarbonate Makrolon 2800 in air.

imum intensities at 375 and 690 nm or 315 and 173 kJ/mol, respectively. The 690 nm band is somewhat structured. The identical spectra of the two dissimilar commercial brands of polycarbonate, which surely differ in nature and amounts of additives (although we did not analyze this and no respective information from the manufacturers is available) suggests that the observed emission phenomena are determined by an intrinsic polycarbonate behavior.

Fluorescence spectroscopy was used to provide further information on this question.

FLUORESCENCE SPECTRA

The fluorescence spectra show that several photo-physical states are intrinsically available in polycarbonate that may lead to photon energies in the ob-

served spectral range. It is not to be expected that the relative intensities of the fluorescence bands are the same as in the peeling spectra, because the stimulation process is completely different. A stimulation process that leads to luminescence spectra, in which the intensities are similar to the peeling spectra, is obtained by electron bombardment (cf. next section).

The polycarbonate for fluorescence spectroscopy samples was purified by precipitation twice and a solvent-cast, isotropic film was formed. The fluorescence spectrum is shown in Figure 5. The excitation spectrum (solid line, labeled "Exc.," left ordinate) is the fluorescence intensity at 550 nm as function of the exciting wavelength. The dashed line (labeled " $r_{Exc.}$," right ordinate) shows the polarization of the excitation spectrum. The fluorescence spectrum (solid line labeled "Flu.") was recorded with an excitation wavelength of 300 nm. The

respective polarization is the dashed line labeled " $r_{Flu.}$."

The essential features of the fluorescence characteristics with respect to the mechanically induced spectra are the increases in the excitation polarization ($r_{Exc.}$) at ~ 350 and ~ 480 nm and the increase in the fluorescence polarization ($r_{Flu.}$) at ~ 630 nm. This indicates that at least three chromophores contribute to the spectra. Chromophore in this relation means photophysical chromophores, i.e., systems of energetic states, which, nevertheless, may be only one chemical species.

MECHANISM FOR THE PHOTON EMISSION CREATED BY DEBONDING

In both the deformed fiber-filled polycarbonate and the polycarbonate film/glass peel experiments, de-

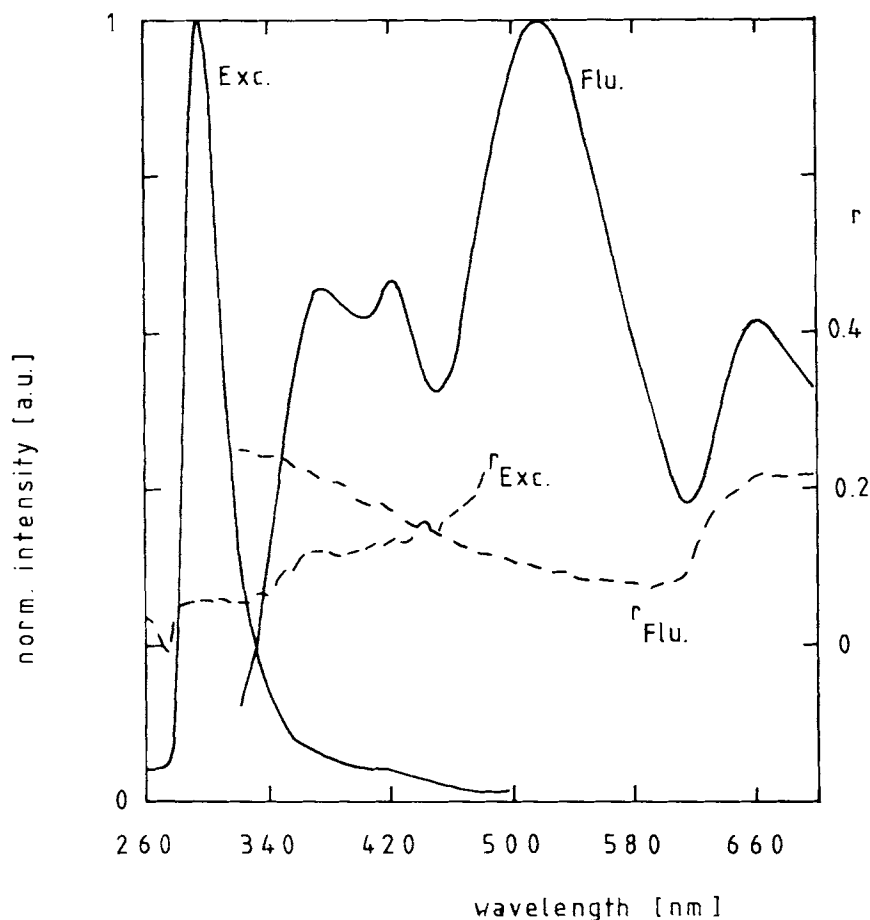


Figure 5 Fluorescence spectrum of polycarbonate: sample: solvent-cast film of bisphenol-A-polycarbonate, Makrolon 2800 purified by reprecipitation twice; (solid line "Exc.") excitation spectrum recorded at a fluorescence wavelength of 550 nm; (solid line "Flu.") fluorescence spectrum recorded at an excitation wavelength of 300 nm; (dashed lines) polarization of the excitation spectrum ($r_{Exc.}$) and the fluorescence spectrum ($r_{Flu.}$).

tachment of the polymer from glass surfaces is occurring. In the first case, due to the large differences in the moduli and the plasticity of the polycarbonate and glass, debonding occurs over a range of gross sample elongation.^{14,15} The consequences of separation between the polycarbonate and glass include large degrees of charge separation (created initially by contact charging) and, potentially, the simultaneous creation of recombination sites, in our case in the polycarbonate near-surface region. During the debonding event, this charge separation creates intense electrical fields that stimulate the motion of charge along the polymer surface. Such motion constitutes the equivalent of electron bombardment of the polymer surface that can stimulate luminescence. The proposed emission mechanism is basically localized electron-positive ion formation, whereupon recombination, it yields photon emission. The very high intensity seen from these interfacial systems is due to the high number of excitations that are generated by the flow of charge occurring during separation.

We can generate a luminescence spectrum by simply bombarding a neat polycarbonate sample with an electron beam (3 keV, 3 mA/cm²) in vacuum. The resulting spectrum is shown in Figure 6. Note that it resembles closely the spectra from both the fiber-filled polycarbonate (internal interfaces) and the peel experiment performed in vacuum. It should also be noted that when the electron beam is removed the polycarbonate surface exposed to the

electron beam continues to luminesce for several seconds.

The tails seen in the photon emission indicate that the polycarbonate surfaces are still *active* in terms of electronic excitations for several seconds after debond. The observed $t^{-\alpha}$ -type decay behavior is really indicative of a dispersive transport process in a complex system.²⁶ This is mathematically equivalent to any process where the kinetics are determined by "excited states," the relaxation of which is coupled to a complex environment with a distribution of relaxation times. This is characteristic of photon emission signals following adhesive failure of a number of composite systems¹⁷ and is in the last step due to the kinetics of recombination of quasi-mobile charge and recombination centers (e.g., mobile electrons and positive ion sites).

CONCLUSIONS

The actual state of research on mechanically induced photon emissions of polycarbonate/glass systems has shown that

- (i) the intense luminescence is a consequence of the cleavage of the polycarbonate/glass interface;
- (ii) it is originated within the polycarbonate; and
- (iii) several chromophores are involved.

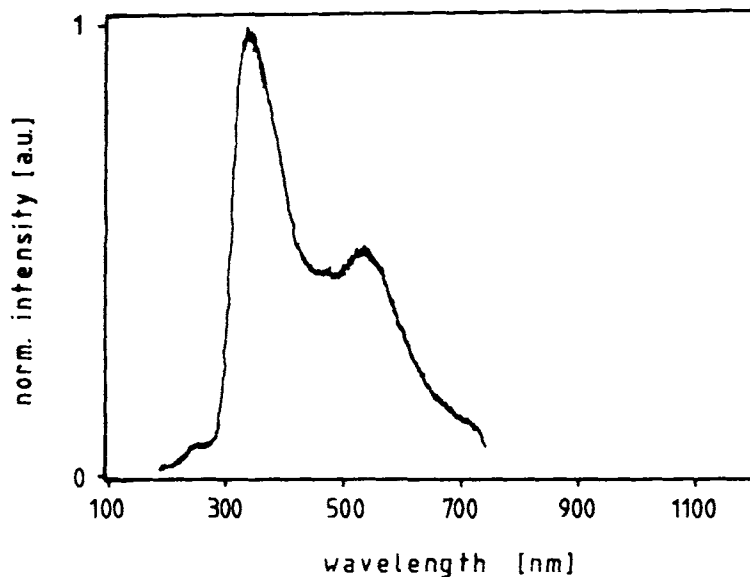


Figure 6 Luminescence spectrum generated by electron bombardment of bisphenol-A-polycarbonate Calibre 300-10 in vacuum.

In general, the use of these emission signals can potentially provide details of failure mechanisms and fracture phenomena, can assist or complement the interpretation of other probes such as acoustic emission, and provide an independent probe of the molecular and microevents occurring prior, during, and after fracture. We have shown that photon emission is sensitive to the locus of fracture in glass-filled polycarbonate, including adhesive failure at embedded interfaces prior to macroscopic fracture of the samples. Our goal is to continue to study the mechanisms and applications of deformation and fracture-induced emissions to the study of early stages of fracture and failure modes in a variety of materials, including neat polymers, composite systems, and interfaces. In addition, we will continue to study the relation of atomic or molecular level events during fracture (which can result in particle and photon emission) with the concepts of energy dissipation with both spatial and temporal resolution. These departures from *adiabatic* separation of atomic planes or molecular bonds are also reflected in the mechanical, topographical, electrical, and chemical states of the resulting surface, generated by deformation or fracture. By correlating and analyzing these properties, we are thus striving to probe the dynamics of the most dangerous type of fracture—catastrophic crack growth—as cracks nucleate, accelerate, arrest, and/or propagate through materials.

We thank M. Hennecke for experimental help and valuable discussions with the fluorescence spectroscopical investigations. Part of the work was supported by the DFG under Grant Ni309/1-1 (postdoctoral visit of L. N. at WSU), by AIF No. 7706, by AFOSR-F49620-91-C-0093, and by the Dow Chemical Co.

REFERENCES

1. H. G. Mosle, K.-H. Lakmann, and B. Wellenkötter, *Kunststoffe*, **73**, 374 (1983).
2. J. Wolters, *J. Acoustic Emission*, **3**, 51 (1984).
3. J. Wolters, private communication.
4. M. A. Grayson and C. J. Wolf, *J. Polym. Sci. Polym. Phys. Ed.*, **23**, 1087 (1985).
5. J. T. Dickinson, L. C. Jensen, S. C. Langford, and R. P. Dion, to appear.
6. J. T. Dickinson, in *Adhesive Chemistry—Developments and Trends*, Ed. L. H. Lee, Plenum Press, New York, 1984, pp. 193–243.
7. J. T. Dickinson, L. C. Jensen, and M. K. Park, *J. Mater. Res.*, **17**, 3173 (1982).
8. S. C. Langford, J. T. Dickinson, and L. C. Jensen, *J. Vac. Sci. Technol. A*, **7**, 1829 (1989).
9. E. E. Tomashevskii and S. Misrow, *Plast. Kautsch.*, **19**, 11 (1972).
10. M. E. J. Dekkers, Thesis, TU Eindhoven, 1985.
11. L. Nick and J. T. Dickinson, to appear.
12. J. T. Dickinson, L. C. Jensen, S. C. Langford, R. P. Dion, and L. Nick, *J. Mat. Res.*, in press.
13. J. H. Golden, *Makromol. Chem.*, **66**, 731 (1966).
14. L. Nick, Thesis, TU Clausthal, 1988.
15. J. Fuhrmann and L. Nick, to appear.
16. K. A. Zimmerman, S. C. Langford, J. T. Dickinson, and R. P. Dion, *J. Polym. Sci.: Polym. Phys. Ed.*, submitted.
17. J. T. Dickinson and L. C. Jensen, *J. Polym. Sci. Polym. Phys. Ed.*, **23**, 873 (1985).
18. J. Fuhrmann and M. Hamel, to appear.
19. J. T. Dickinson, in *Non-Destructive Testing of Fibre-Reinforced Plastics Composites*, Ed. J. Summerscales, Elsevier, Essex, 1990, Vol. 2, pp. 429–482.
20. J. T. Dickinson, in *Adhesive Bonding*, Ed. L. H. Lee, Plenum Press, New York, 1991, pp. 395–423.
21. R. W. Rendell, K. L. Ngai, G. R. Fong, A. F. Yee, and R. J. Bankert, *Polym. Eng. Sci.*, **27**, 2 (1987).
22. M. Zhen-Yi, F. Jiawen, and J. T. Dickinson, *J. Adhesion*, **25**, 63 (1988).
23. A. S. Crasto, R. Corey, J. T. Dickinson, R. V. Subramanian, and Y. Eckstein, *Compos. Sci. Techn.*, **30**, 35 (1987).
24. M. Zhen-Yi and J. T. Dickinson, *J. Appl. Phys.*, **70**, 4797 (1991). M. Zhen-Yi and J. T. Dickinson, *Macromol. Chem. Macromol. Symp.*, **41**, 9 (1991).
25. K. A. Zimmerman, S. C. Langford, and J. T. Dickinson, *J. Appl. Phys.*, **70**, 4808 (1991).
26. H. Sher, M. F. Shlesinger, and J. T. Bendler, *Phys. Today*, **44**, 26 (1991).

Received April 10, 1992

Accepted September 28, 1992